THERMAL DISTORTION ANALYSIS OF A
DEPLOYABLE PARABOLIC REFLECTOR

By Lloyd R. Bruck and George H. Honeycutt

NASA Goddard Space Flight Center

SUMMARY

The Goddard Space Flight Center has performed a thermal distortion analysis of the Advanced Technology Satellite (ATS-F) 9.144m (30 ft.) diameter parabolic reflector using NASTRAN Level 15.1. The same NASTRAN finite element model was used to conduct a 1g static load analysis and a dynamic analysis of the reflector. In addition, a parametric study was made to determine which parameters had the greatest effect on the thermal distortions. This paper describes the method used to model the construction of the reflector and presents the major results of the analyses.

INTRODUCTION

The ATS-F is the latest in a series of spacecraft designated as Advanced Technology Satellites. This 3-axis stabilized synchronous satellite has been designed as a multiple mission system to allow for numerous communications, meteorological and scientific studies.

The ATS-F spacecraft is shown in the launch configuration in Figure 1 and in the orbital configuration in Figure 2. The predominate feature of the spacecraft is a 9.144m (30 ft.) diameter parabolic dish high gain antenna. The success of many of the spacecraft experiments depends on maintaining the design surface contour of the parabolic reflector after deployment. In addition, the spacecraft control system must adhere to stringent pointing and slewing requirements for R-F beam positioning.

The surface contour of the reflector is distorted in orbit by the thermal environment of space. It is necessary to predict what these distortions will be in order to assess the R-F performance of the reflector. As there is no practical or realistic ground test that will provide this data it was necessary to resort to analytical methods. Accordingly, GSFC has performed a thermal distortion analysis of the ATS-F reflector using NASTRAN Level 15.1 for selected thermal load cases that produces the required reflector distortions.

As a partial check on the validity of the NASTRAN model a 1g static deflection analysis was also accomplished. The results

103

were compared with an actual measurement of the 1g deflections to provide some information on the accuracy of the model.

To help determine which parameters were most important in controlling the thermal distortions, a parametric study was made. In this study the effects of the mesh, rib temperature, and rib thermal gradients were varied to determine the relative magnitude of the effects on the thermal distortions.

In addition, the fine pointing and slewing requirements necessitated obtaining the dynamic characteristics of the reflector. With only slight modification to the static NASTRAN model the first natural frequency and mode shape were obtained to provide information for design of the control system.

The prime contractor for the ATS-F spacecraft is Fairchild Space and Electronics Company; the subcontractor for the parabolic reflector is Lockheed Missiles and Space Company. Both of these organizations provided information which made these analyses possible.

REFLECTOR DESCRIPTION

General

The deployed reflector is composed of 48 flexible ribs hinged to the spacecraft hub at 7.5 degree increments as shown in Figure 2. A woven copper coated dacron mesh serves as the reflective surface and is connected between each rib at the top edge of the rib. When stored for launch, the ribs are wrapped around the hub with the mesh carefully folded between the ribs. The packaged reflector is enclosed by a series of doors that are secured by a circumferential restraining cable. When the restraining cable is severed, the elastic energy stored in the ribs is released causing the ribs to unwrap to the deployed position. During deployment the ribs pivot freely about the hinges at the hub; when fully deployed the hinges are locked. The reflector is designed so that there is always a small tension load acting on the mesh keeping it taut during orbit.

Rib Description

An individual reflector rib is shown in Figure 3. The rib tapers in width from its attachment at the hub to the outer edge of the reflector. The cross section of the rib normal to the parabolically curved principal axis is of semi-lenticular shape and also varies along the rib. Each rib is made from a single piece of aluminum sheet with varying diameter holes cut out along its length. The holes are provided to permit the heat input from the sun to pass freely through the rib to prevent excessively

104

severe thermal gradients.

Mesh Description

The R-F reflective mesh is constructed from copper coated dacron yarn bundles overcoated with a thin silicone sealant. The warp yarn running in the longitudinal direction (radially along the rib) is made from double strand dacron, 10 pair/cm while the filling yarn in the transverse direction (circumferential from rib-to-rib) is made from single strand dacron 12.5 strands/cm. This form of construction makes the woven mesh behave nonisotropically and consequently have material properties (modulus of elasticity and the thermal coefficient of expansion) that differ in each principal direction. Tests on the mesh have revealed that Poisson's ratio is essentially zero for this material in both directions indicating that the yarns in either direction behave independently of one another when each is loaded individually.

Hub Description

The aluminum hub, Figure 4, is composed of two ring sections connected every 7.5 degrees by risers located midway between each rib. The reflector is protected in the folded position by a cover as shown in Figure 4. This cover provides no significant load carrying structure to the hub. The rib hinge attachment to the hub is also illustrated.

Attachment of the hub to the spacecraft is provided by the mounting assembly indicated in Figure 5. This assembly, located every 90 degrees, provides for a rigid attachment of the hub to the spacecraft except for the rotation that is allowed to take place at the hinge. The purpose of this method of attachment is to assist in the isolation of the antenna from any structural motion created by the spacecraft.

FINITE ELEMENT MODEL

Rib Model

The finite element model of the rib is shown in Figure 6 where each of the 48 ribs have been represented by 10 bar elements making a total of 480 rib elements. A significant feature of the rib model is that the offset between mesh attachment point and the rib centroidal axes is retained. The effect of this offset is to introduce a twisting moment about the rib longitudinal axis when the rib is loaded in the lateral (circumferential) direction by mesh loads and a bending of the rib about a circumferential axis when loaded in a radial direction by the mesh. This offset is shown in Section A-A of Figure 6.

The shear center of the rib and the rib centroidal axis do not coincide. Prior to the formulation of the 10 element rib model a much more detailed plate element model of a single rib was generated which simulated the shear center offset. Various thermal gradients were applied to this model to determine the resulting twist and warp of the rib. The results of this analysis indicated that the offset shear center causes only slight twist and warp of the free rib. Because the mesh would act to resist the twist of the rib, the restraining force of the mesh would tend to further minimize the effect of twist or warp on the thermal deformations. Therefore, it was concluded the effect of the shear center offset is minimal and can be neglected.

The reflector deflection resulting from thermal or gravitational loads is determined for grid points at the mesh attachment point to the rib.

Hinges are provided at the hub for attachment of the ribs to the hub and to allow the ribs to rotate to their fully deployed configuration. These hinges become fixed at deployment. For this reason the rib hinges were fixed in the model.

Mesh Model

The reflector mesh has been modeled by membrane elements capable of carrying in-plane tension loads. Each mesh section between ribs has been subdivided into 10 trapesoidal membranes that are attached to each corner to the grid points located at the rib edge. The nonisotropic properties of the mesh have been reflected in the model parameters; the mesh thermal coefficients of expansion and modulus of elasticity are given as functions of temperature.

Hub Model

The hub is modeled with bar elements as shown in the hub segment depicted in Figure 7. A centroidal axis offset of the upper and lower hub rings at the hinge has been provided in order to position the hinge elements in their proper location. Four attachment points are provided for securing the hub to the spacecraft. This attachment allows rotation of the hub in the direction of the hinges as in the actual construction by using the pin flag option in NASTRAN.

COMPLETE FINITE ELEMENT MODEL

The complete finite element model, Figure 8, is composed of the hub, mesh, and rib models discussed previously. This figure was obtained by using the plot module of NASTRAN. A total of 1404 elements connected between 728 grid points are used to model the complete reflector. As every grid point is allowed to

ave 6 degrees of freedom, with the exception of 4 grid points
that are fixed simulating the spacecraft, there are 4,344 total
degrees of freedom.

In the static analysis the decomposition of the stiffness
matrix (semi-bandwidth of 15 terms with 87 active columns and 14
rows) consumed the bulk of the computer time. Run time using
standard core on the IBM 360-95 for one static load case was 15
minutes, 10 minutes of which was used decomposing the stiffness
matrix.

In the dynamic analysis, using the inverse method eigen-
value extraction routine, obtaining one eigenvalue used about 35
minutes of the total run time of 38 minutes.

1g ANALYSIS

A 1g load in the -Z direction was placed on the reflector
in order to check out the finite element model and to provide a
comparison with static deployment test results of the actual
reflector. Reflector deflection results are presented as plots
of the vertical (Z) deflection of the rib tip at 4.572m (180 in.)
radius versus rib number. Figure 9 illustrates the rib numbering
system. The 1g NASTRAN result and actual test results are compared
in Figure 10. This comparison indicates good agreement with the
actual test results was achieved.

ORBITAL THERMAL DEFLECTION ANALYSIS

Thermal Load Input

A reference temperature of 294°K (70°F) was assigned to each
element to define the as-assembled temperature. Orbital tempera-
ture distribution for the various orbit hours served as the thermal
load input for the finite element model. The temperatures for each
rib segment (10 segments per rib) were determined for an upper node
(T_1) and a lower node (T_2). These temperatures were averaged in
the GSFC analysis to define the temperature assigned to the rib
element in the longitudinal direction. The rib gradient across
the rib was calculated using $(T_1-T_2)/d$ where d is the distance
between the upper and lower nodes (see Figure 11). Each mesh
element and each grid point was assigned a temperature; for those
grid points where nodal temperatures were not defined a linear
interpolation was made.

The effect of the spacecraft attachment to the deployed
reflector is presented by a set of initial displacements at the
four attach points.

Thermal Deflection Results

Although the deflection results for 12 orbit hours were determined, only those resulting from orbital thermal loads developed during orbit hours 5, 12, and 24 for Beta =0° will be presented as they provide a representative sampling of the total results. Figure 12 presents the satellite orientations for various orbit hours and defines the orbit angle Beta.

• Orbit Hour 12, Figure 13 ⁻ The reflector is completely shaded by the earth and is very cold. The shrinkage of the reflector caused the rib tips to deflect to their maximum value.

• Orbit Hour 24, Figure 1₄ ⁻ The reflector sees its least severe thermal load. As a consequence its deflections are a minimum.

• Orbit Hour 5, Figure 15 ⁻ One half of the reflector is shaded by the other half. Because of this effect, the thermal gradient developed across the rib is relatively large and takes the shape plotted in Figure 16. Note that the plot of the thermal gradient across the rib corresponds closely to the plot of the deflected shape of the reflector; compare Figures 15 and 16.

PARAMETRIC VARIATION STUDY

In an effort to determine the relative effect of various model parameters on the deflection of the reflector, a parametric variation study was conducted on the finite element model. The temperature distribution present during orbit hour 5, Beta=0 was used for the five cases investigated.

Case 1 - This case determined the reflector deflection with the mesh removed and with the thermal gradient across the width of the rib set equal to zero. The resultant deflection, Figure 17, is caused by the rib temperatures and radial rib gradient only and is relatively small.

Case 2 - The mesh has been removed and only rib temperatures and gradients are present, both radially along the rib axis and across the width of the rib. The results of this variation are shown in Figure 18. Note that the deflections are large and the shape of the plot of the rib deflections again agrees, as expected with the shape of the plot of the average depthwise temperature gradient as shown in Figure 16.

Case 3 - The radial mesh elements have been removed and only circumferential mesh elements are present. The rib temperatures and radial temperature gradient are present along the rib, but the gradient across the width of the rib has been set equal to zero. Deflection results are shown in Figure 19. Although there are

major differences in the temperature distribution around the circumference of the reflector ranging from 116°K (-251°F) to 269°K (25°F), the net effect on the mesh is that a uniform tension is created in each circumferential band. This statement is substantiated by the results which indicate a uniform deflection is created at the outer edge of the reflector.

Case 4 - The circumferential mesh elements have been removed and there is no depthwise rib gradient; the radial mesh elements remain, as well as the rib temperatures and radial rib gradients. Figure 20 presents the results. The net effect of the radial mesh can be obtained from subtracting Case 1 results from this case, Case 4. It would appear that the deflections caused by the radial mesh element are insignificant for this case.

Case 5 - The effect of varying the depthwise rib gradient is shown in Figure 21. The results of 3 parametric changes are shown: no gradient, actual gradient, and 3 times the actual gradient. The major impact the rib gradient has on the deflection is evident.

DYNAMIC ANALYSIS

The finite element model was used to determine the first torsional frequency of the deployed reflector. Comparison of the NASTRAN result of 1.18 Hz with a value obtained from a modal survey test of 1.15 Hz indicates good agreement.

A motion picture of the torsional mode was obtained by the proper adjustment of the amplitude in repeated plots of the modal displacements in the plot routine and repeating them sequentially on 16mm film.

CONCLUSION

NASTRAN has proven to be a most valuable tool in conducting the thermal distortion analysis. Because of the capability built into NASTRAN the parametric study was easily accomplished by the alteration or addition of a few input cards The value of the data obtained far outweighed the cost of the additional computer time required. The results of this analysis supplied valuable information on the performance characteristics of the parabolic antenna and provided insight into the structural interactions of the various parts of the reflector.

The results of the 1g analysis compared favorably with available test results which provided some confidence that the model was satisfactory. Again with but a few card changes and using a different rigid format the first torsional natural frequency and mode shape were obtained.

The addition of a beam element capable of handling the offset shear center effect would have saved the considerable time and effort expended to prove it had little effect in this problem. It is recommended that this capability be added to NASTRAN.

ACKNOWLEDGEMENT

110

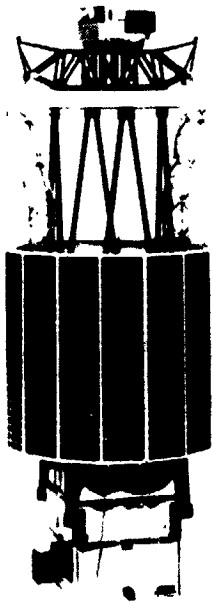Figure 1. ATS-F Launch Configuration
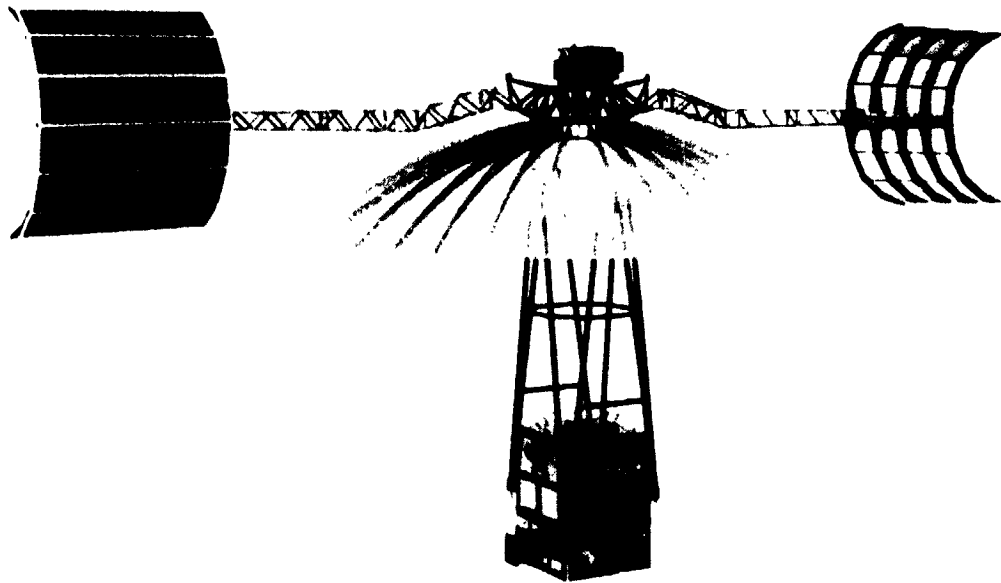
Figure 2. ATS-F Orbital Configuration

111

HINGE END

TIP END

Figure 3. Reflector Rib

UPPER RING

RISER

LOWER RING

DOOR

FOLDED RIB-MESH PACKAGE

COVER
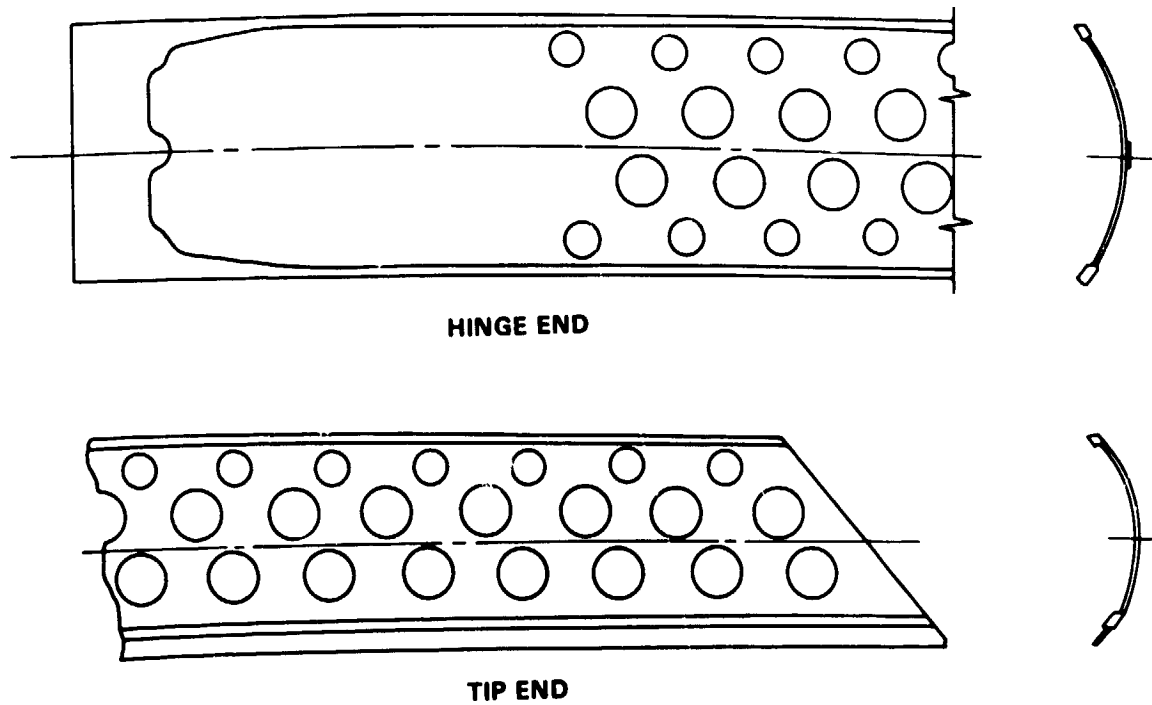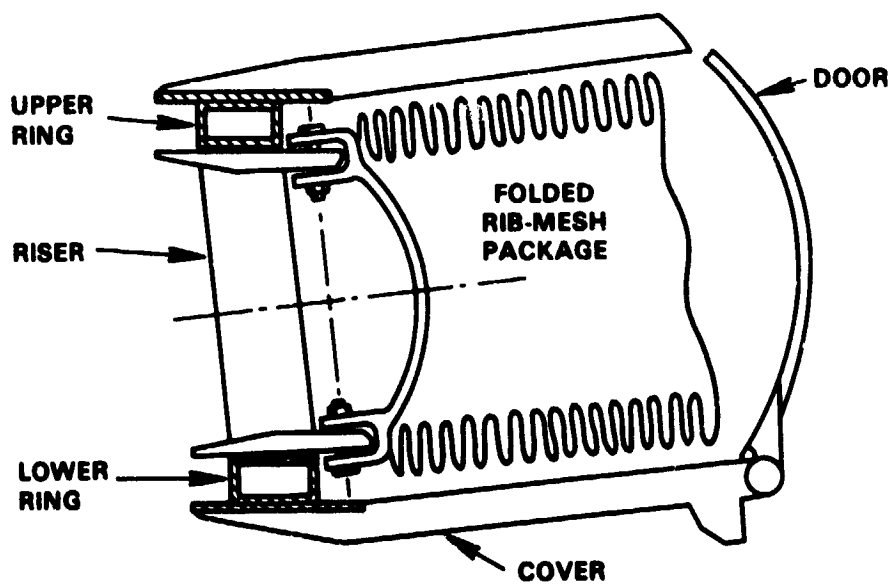
Figure 4. Hub Cross-Section and Rib Hinge

112

HUB RING

HINGE LINE

MOUNTING BRACKET

UPPER RING

RISER

RISER

LOWER RING
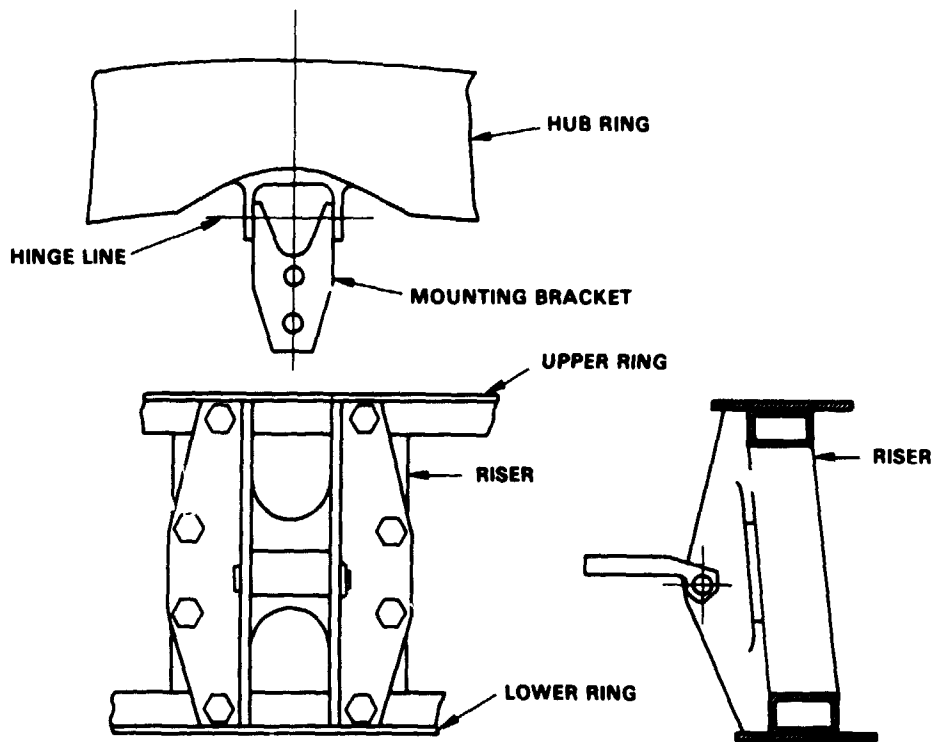
Figure 5. Reflector/Spacecraft Attachment

GRID POINT AT
MESH ATTACH POINT

OFFSET

SHEAR CENTER

OFFSET

SECTION A-A

A

MESH CONTOUR

A

GRID POINT
OFFSET DISTANCE

RIB ELEMENT

HUB HINGE
GRID POINTS

RIB CENTROIDAL AXIS

Figure 6. Rib Model

113
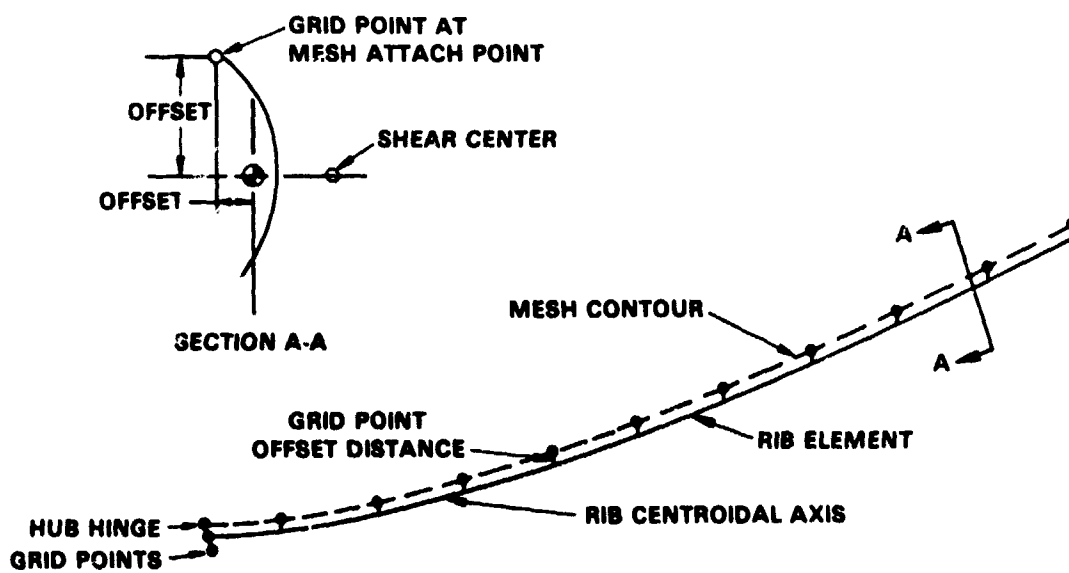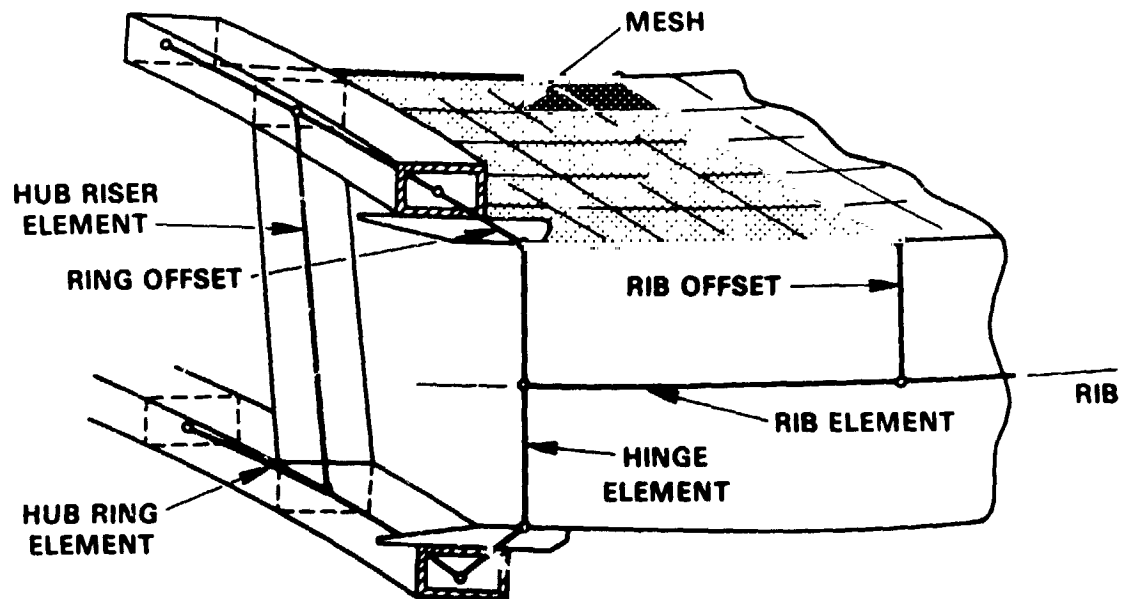
Figure 7. Hub Model
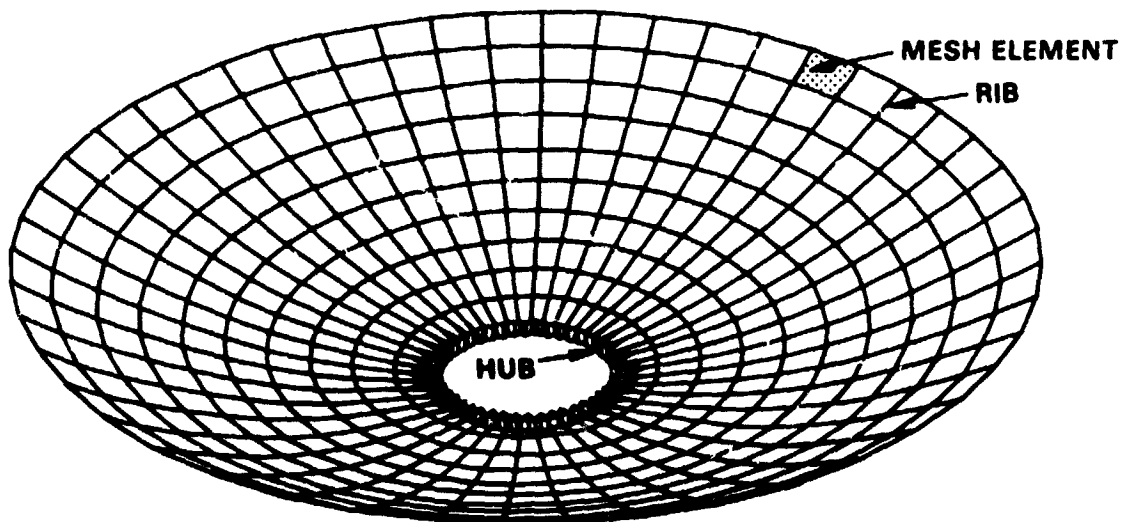
728 GRID POINTS
480 MESH ELEMENTS
480 RIB ELEMENTS
432 HUB ELEMENTS
  12 ATTACH POINT ELEMENTS
1,404 TOTAL ELEMENTS

Figure 8. Complete Finite Element Model

114
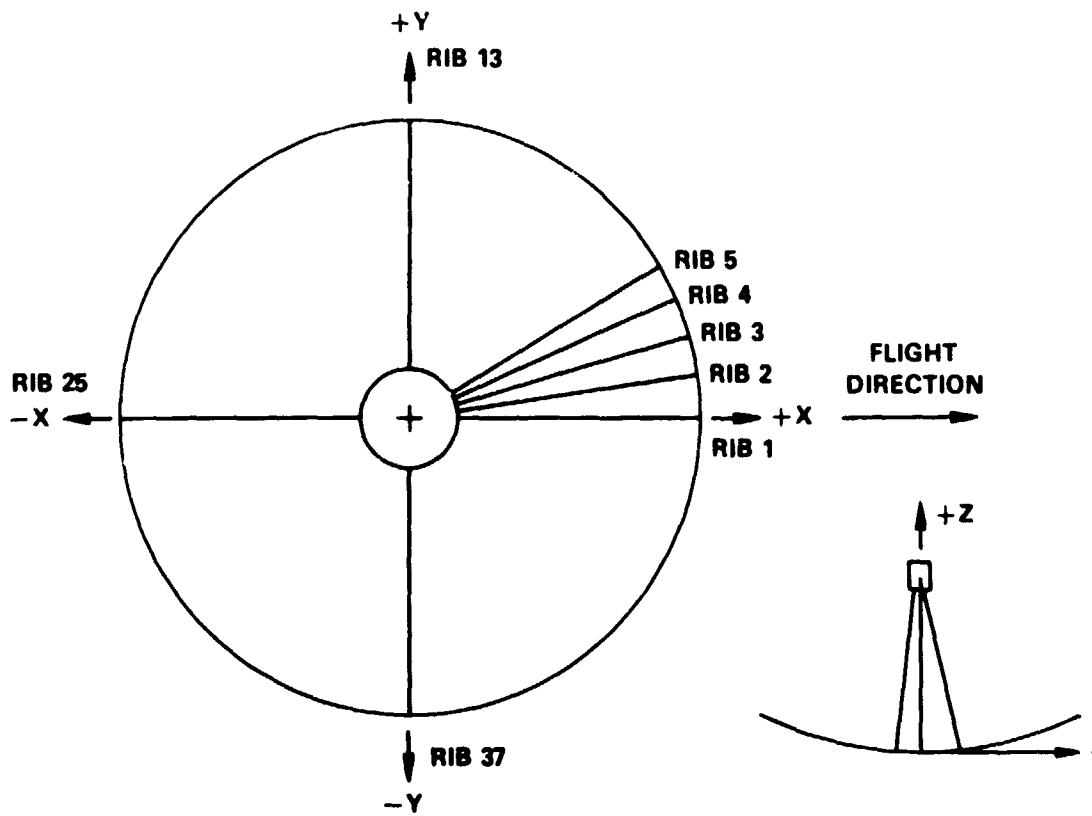
Figure 9. Reflector Rib Locations
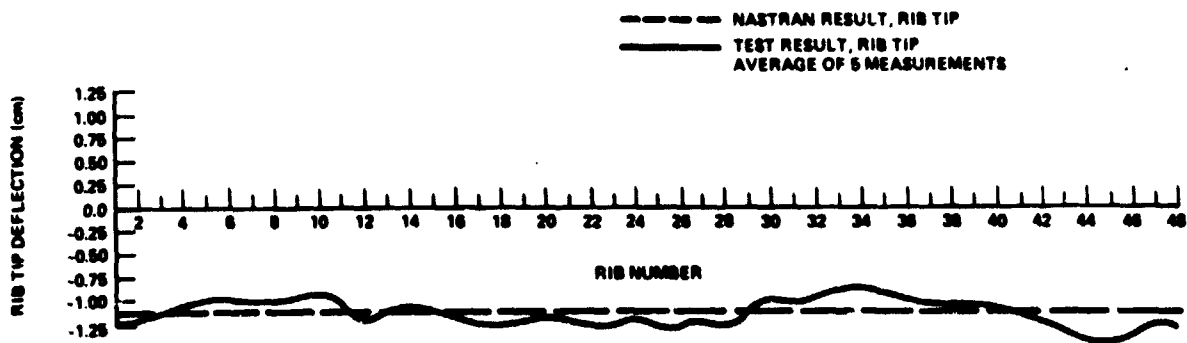
Figure 10. Rib Deflection 1g Analysis

THERMAL GRADIENT $\dfrac{T_1 - T_2}{d}$
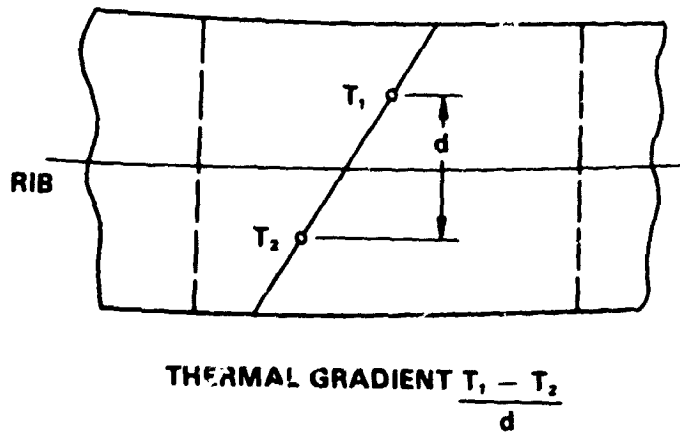
Figure 11. Rib Depthwise Thermal Gradient

NOTE: BETA IS THE ANGLE BETWEEN
THE ORBITAL PLANE & THE SUN.
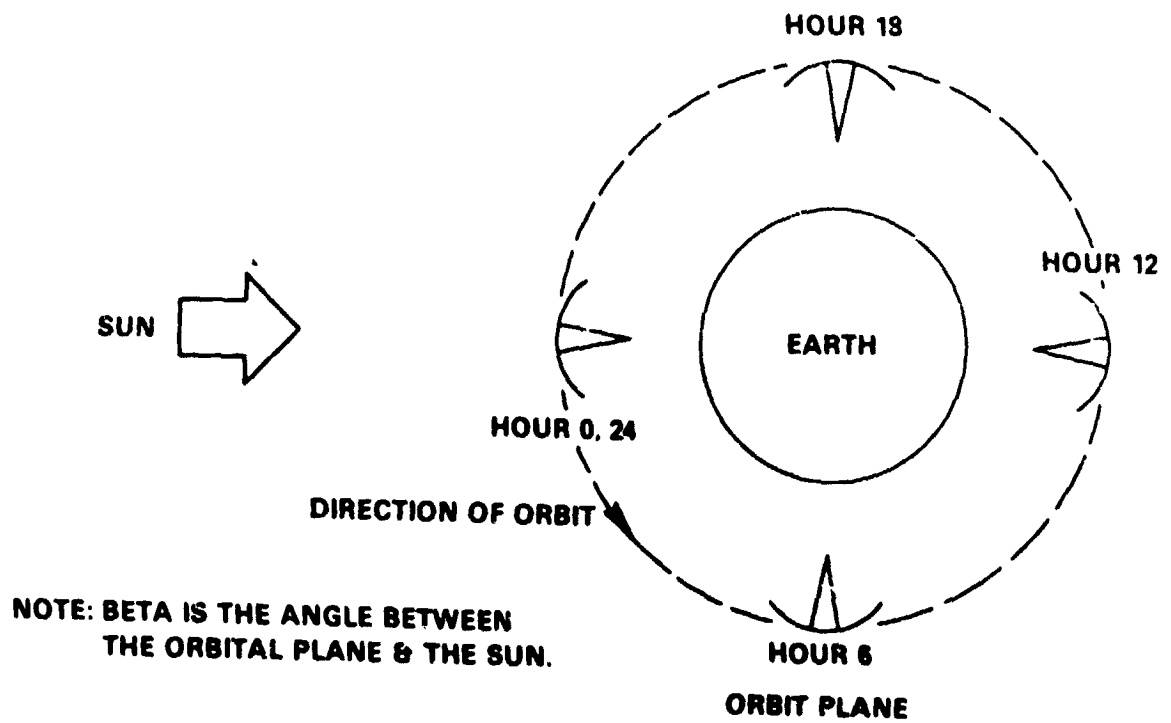
Figure 12. Sun-Earth-Spacecraft Orientations

RIB DEFLECTIONS PLOTTED AT:

———————— r = 456 cm (180 in.)
— - — - — r = 344 cm (135 in.)
· — · — · r = 231 cm (91 in.)

RIB NUMBER
RMS = 1.32 cm (.52 in.)
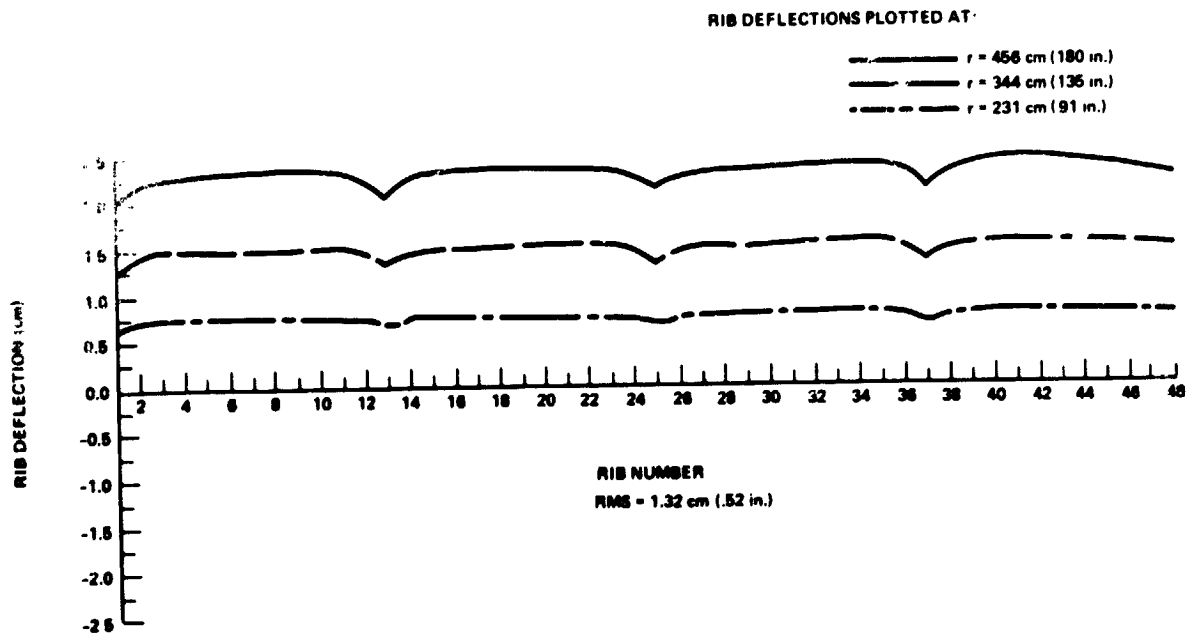
Figure 13. Rib Deflection Orbit Hour 12 Beta=0°

RIB DEFLECTIONS PLOTTED AT:

———————— r = 456 cm (180 in.)
— — — — r = 344 cm (135 in.)
— · — · — r = 231 cm (91 in.)

RIB NUMBER
RMS = 0.25 cm (0.10 in.)
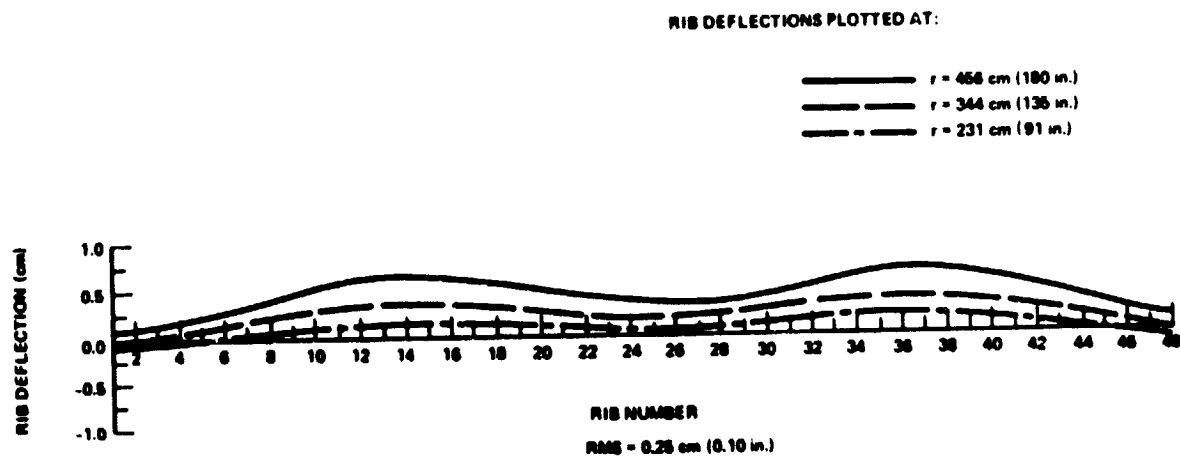
Figure 14. Rib Deflection Orbit Hour 24 Beta=0°

117

RIB DEFLECTION PLOTTED AT.

———————— r = 456 cm (180 in)
—— —— —— r = 34⁴ ⁻m (135 in)
—— —— —— r = 231 cm (91 in)
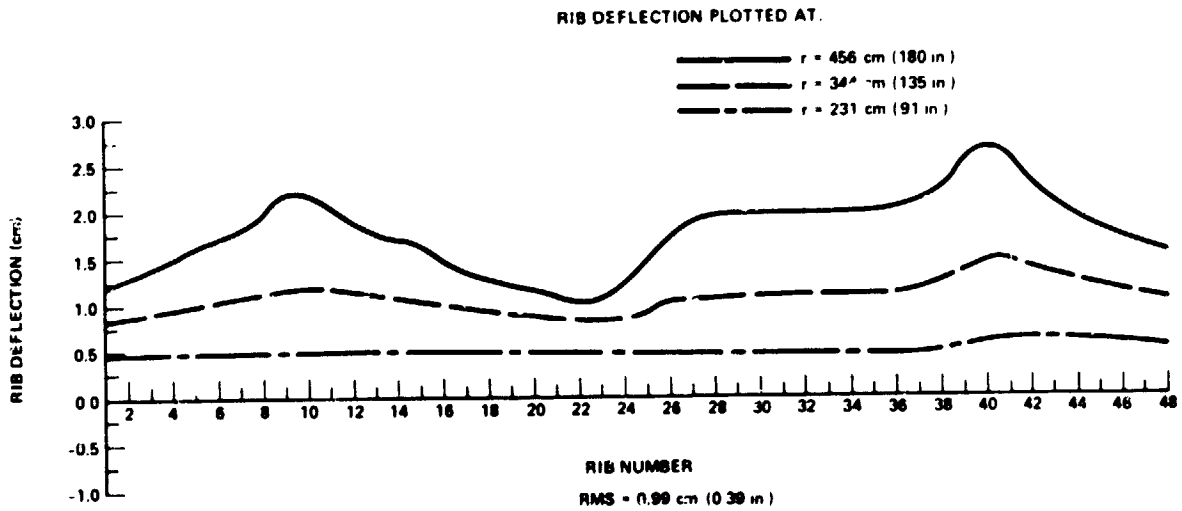
Figure 15. Rib Deflection Orbit Hour 5 Beta=0°
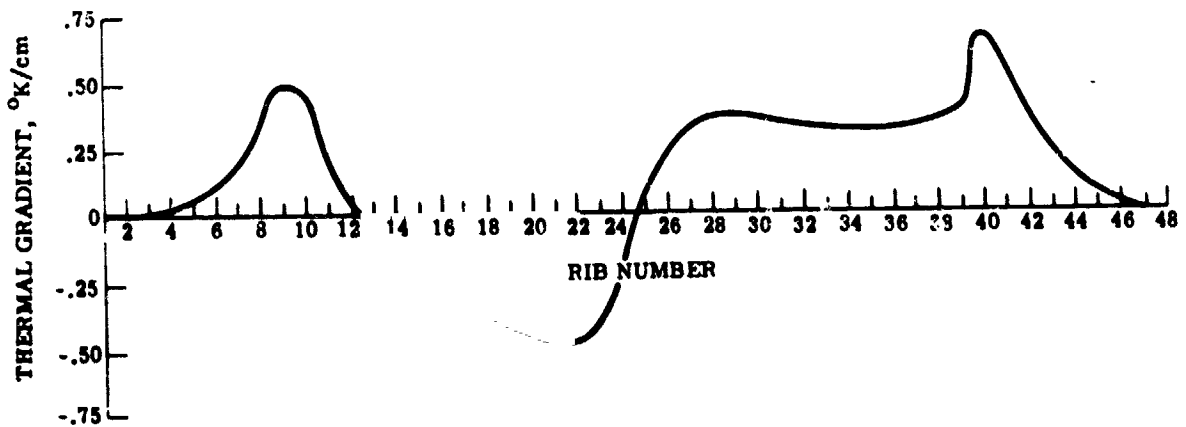
Figure 16. Average Depthwise Thermal Gradient
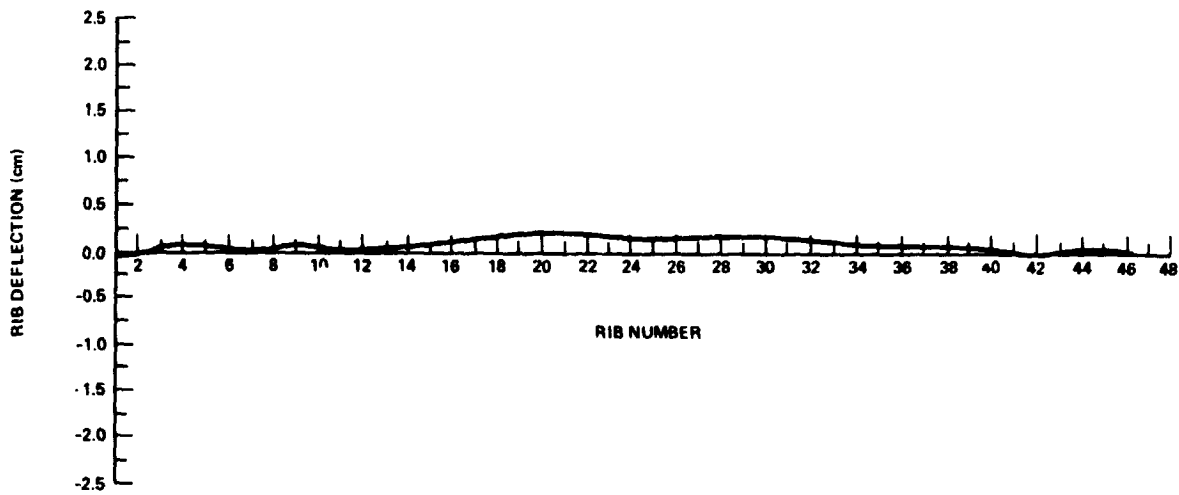Orbit Hour 5 Beta=0°

118

Figure 17. Case 1 — Effect of Rib Temperatures
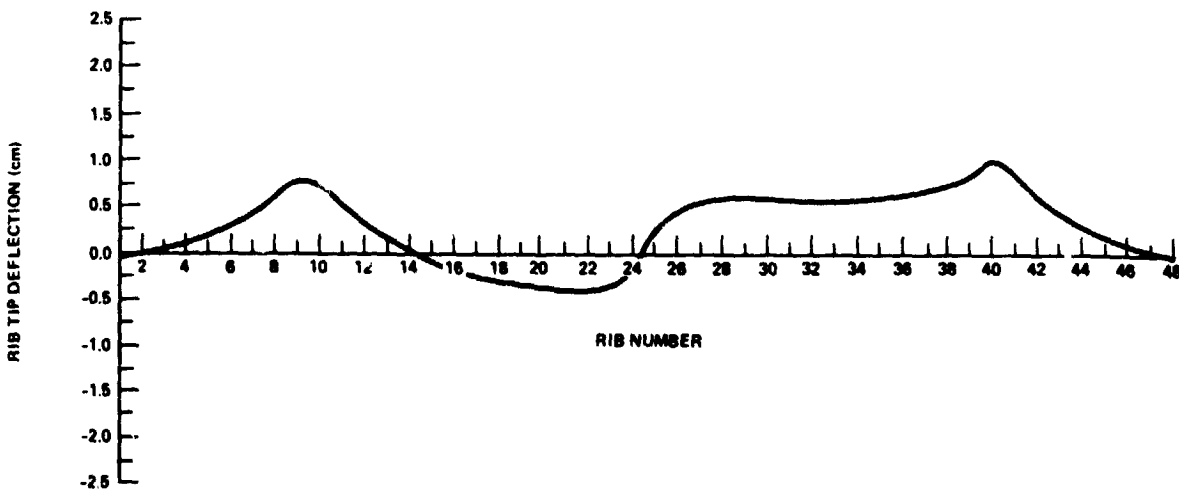Orbit Hour 5 Beta = 0°
No Mesh, No Depthwise Rib Gradient

Figure 18. Case 2 — Effect of Depthwise Rib Gradients & Rib Temperatures
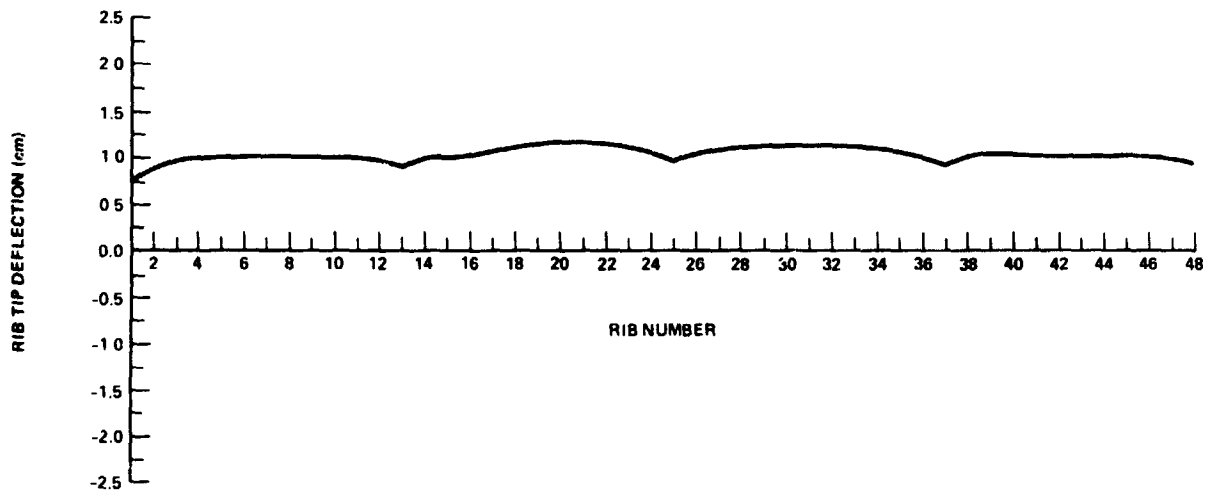Orbit Hour 5 Beta - 0°
No Mesh

119

Figure 19. Case 3 — Effect of Circumferential Mesh
Orbit Hour 5 Beta = 0°
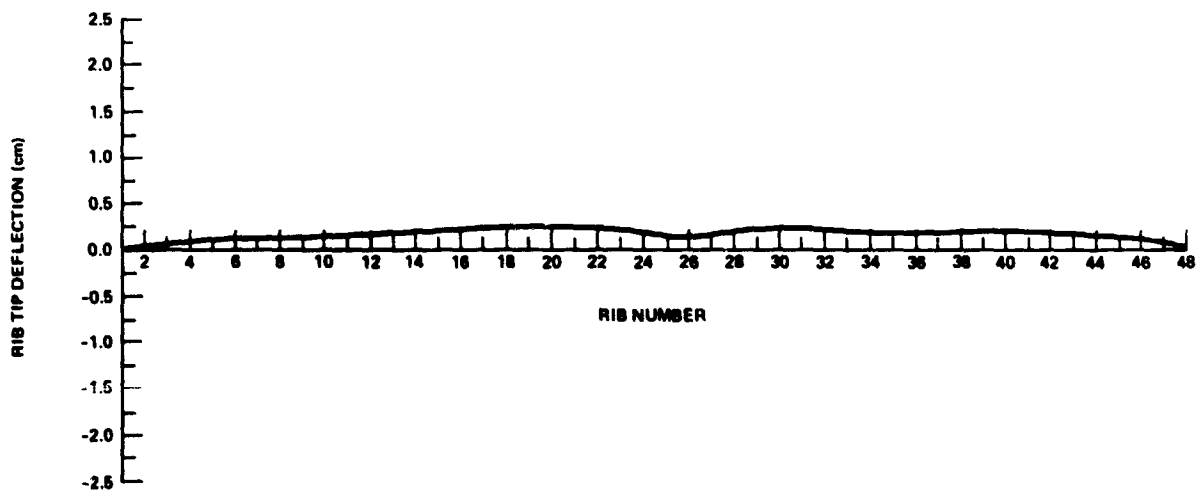No Radial Mesh, No Depthwise Rib Gradient

Figure 20. Case 4 — Effect of Radial Mesh
Orbit Hour 5 Beta = 0°
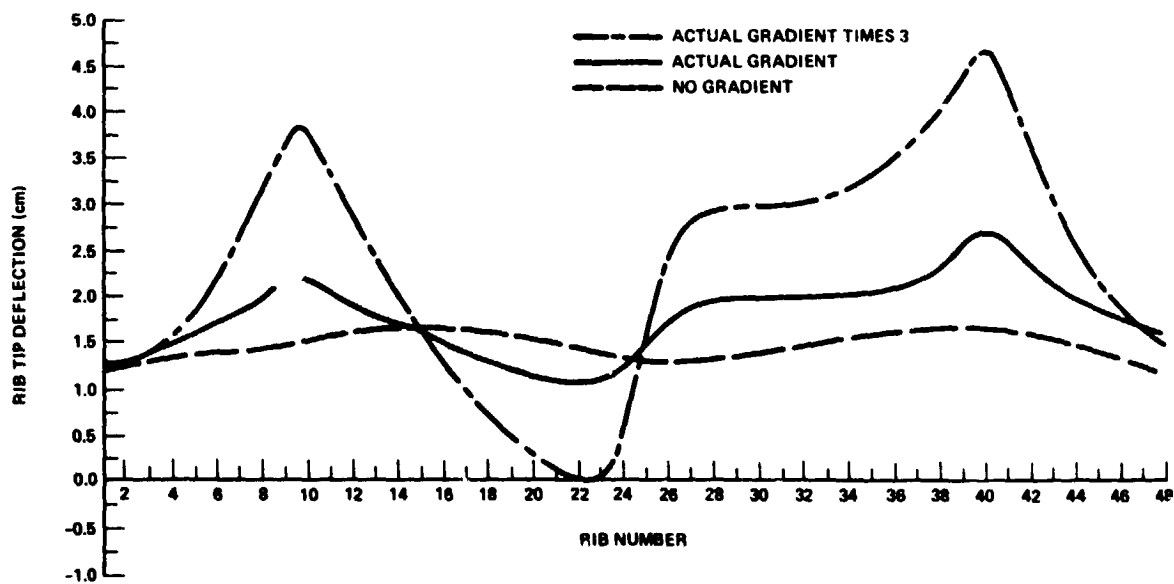No Circumferential Mesh, No Depthwise Rib Gradient

120

Figure 21. Case 5 — Effect of Varying Depthwise Rib Gradient
Orbit Hour 5 Beta=0°